

# NUMERICAL AND EXPERIMENTAL ESTIMATION OF SHRINKAGE CAVITIES DURING Al-ALLOYS CASTING

Adnan S. Jabur  
Engineering College  
University of Basrah

Farhad M. Kushnaw  
Materials Eng. Department  
University of Technology

Imad A. Hussain  
Materials Department  
University of Baghdad

## ABSTRACT

The aim of this research is to predict the shrinkage defects in Al-Si castings by determination the suitable parameters and techniques which can be applied in casting simulation system. Also, it aims to specify the role of silicon content in amount, morphology, and distribution of these defects. The Numerical solution has been carried out using an explicit 3-D finite difference method for the given system of the casting and a mold. Additionally, an experimental casting of the studied samples was achieved. It was found that the shrinkage porosities increased with increasing the silicon content up to 7%, so at this peak, they spread in all cast regions and cannot be predicted. The low silicon alloys suffered from only the shrinkage cavities defects that can be predicted by mapping the solidus time contours. Finally, it was concluded that the critical temperature gradient value of the porosities development in the eutectic (Al-12%Si) alloys was 1.3 °C/cm.

## التقدير العددي والتجريبي لفجوات التقلص خلال سبائك الألمنيوم

د. عدنان أحمد حسين  
كلية الهندسة/ جامعة بغداد

د. فرهاد محمد عثمان  
قسم هندسة المواد/ الجامعة التكنولوجية

د. عدنان شمخي جبر  
كلية الهندسة/ جامعة البصرة

## الخلاصة

ان الهدف من هذا البحث هو تخمين عيوب الانكماش في مسبوكات الألمنيوم-سليكون وذلك بتحديد المعاملات والتقنيات المناسبة التي يمكن تطبيقها في نظام محاكاة السبائك. و يهدف ايضا لتحديد دور محتوى السليكون في كمية و شكل وتوزيع هذه العيوب. نُفذت الحلول العددية باستخدام طريقة الفروق المتناهية ثلاثية الأبعاد، للمسبوكة والمقابل. كذلك تم تحضير العينات المدروسة مخبريا. ولقد وجد ان مسامات التقلص تزداد مع زيادة محتوى السليكون والى حد 7% حيث تنتشر في جميع مناطق المسبوكة ولا يمكن تخمينها. تعاني السبائك قليلة السليكون من الفجوات فقط والتي يمكن التنبؤ بها برسم خطوط زمن التجمد. واختتمتم التوصل الى ان قيمة التدرج الحراري الحرجة لظهور المسامات في السبائك اليوتكتيكية (Al-12%Si) تساوي 1.3 °C/cm.

**KEYWORDS:** simulation, Al-Si alloys, casting structures, numerical analysis, shrinkage defects

## INTRODUCTION

Producing sound aluminum-silicon castings is one of great economic significance to the foundry industry; however, shrinkage defects are the main categories of casting defects which take many forms; shrinkage cavity, porosity and surface sink. Such defects have a negative economic impact on casting production; their consequences range from

high rework costs to casting rejection as reported by Beckermann [1].

During recent years, the application of some popular commercial software as computer simulation tools has become widely accepted within the foundry industry. The application of casting simulation has been most beneficial, for avoiding shrinkage scrap, by predication of shrinkage defects without having to discover them in the foundry through

the usual trial and error process, which can be very tedious, time consuming, and expensive. One of the methods to describe solidification modeling is the heat transfer model, which solves the energy equation. There have been few studies to model the effect of solidification shrinkage from different perspectives. Trovant and Argyropoulos [2] proposed an algorithm to account for shrinkage and consequently determine the shrinkage profile resulting from phase and density change. Only the energy equation is solved in the domain and the effects of solidification shrinkage are imposed through the proposed algorithms. McBride [3] presented a model that accounts for shrinkage during the directional solidification or dendritic binary alloy under the assumption that the densities of liquid and solid phase are different but constant. Also, Kim and Ro [4] performed a study on shrinkage formation during solidification of a material in a two-dimensional rectangular cavity. Anderaus and Delli'isola [5] proposed a 2-D finite difference model to describe the influence of solidification shrinkage on the final shape of cast ingot. Fard [6] develops a numerical method to simulate the solidification shrinkage of the solidifying liquid.

The aim of this work is to find the suitable criteria or methods that can be used in prediction the shrinkage defects. Also, it aims to study the effect of silicon content on the morphology, quantity, and distribution of the shrinkage defects in the Al-Si castings.

## MATHEMATICAL MODEL

### Metal Region

The variation of temperature  $T$  with time could be described by solving the Fourier heat equation, which is generally written as:

$$\rho C_p \left( \frac{\partial T}{\partial \tau} \right) = K \left[ \left( \frac{\partial^2 T}{\partial x^2} \right) + \left( \frac{\partial^2 T}{\partial y^2} \right) + \left( \frac{\partial^2 T}{\partial z^2} \right) \right] + \dot{q} \quad \dots 1$$

where convection is neglected. The density denotes as  $\rho$ , specific heat of casting as  $C_p$  and the term  $\rho C_p (\partial T / \partial \tau)$  is the transient term where,  $\tau$  is a time step. In the right side the three terms represent the heat conduction in three-

direction with thermal conductivity  $K$ . A source term  $\dot{q}$  is an internal heat generation for solidification under equilibrium condition. This term can be described as:

$$\dot{q} = \rho L \frac{\partial f_s}{\partial \tau} = \rho L \frac{df_s}{dT} \frac{dT}{d\tau} \quad \dots 2$$

where  $L$  denotes latent heat distributed over the solidification range, so it is a function of the solid fraction as confirmed by Poirier and Salcedean [7].

Thermophysical properties in the mushy region will depend upon the amount of liquid and solid (i.e. solid fraction) and can be calculated as following:

$$P_T = f_{s(T)} P_{sol} + (1 - f_{s(T)}) P_{liq} \quad \dots 3$$

where  $f_{s(T)}$  are the solid fraction at  $T$  and  $P_{sol}$  and  $P_{liq}$  are values of the property at solidus and liquidus temperatures, respectively.

If the alloy has very narrow solidification interval or it is a pure metal or a eutectic,  $T_s$  will be close to or equal to  $T_L$ . In this case an artificial temperature interval has to be assumed. This temperature interval should be as small as possible to be near the real material behavior.

$$f_l = \left( \frac{T - T_s}{T_l - T_s} \right) \quad \dots 4$$

### Mold Region

For heat conduction in the mold, the energy equation is:

$$\rho_m C_m \left( \frac{\partial T_m}{\partial \tau} \right) = K_m \left[ \left( \frac{\partial^2 T_m}{\partial x^2} \right) + \left( \frac{\partial^2 T_m}{\partial y^2} \right) + \left( \frac{\partial^2 T_m}{\partial z^2} \right) \right] \quad \dots 5$$

the subscript  $m$  is denoted the mold and  $K_m$  is the mold material thermal conductivity.

### Boundary Conditions

On the outer surface, heat transfer is done by convection as following:

$$-K_m \frac{\partial T_m}{\partial x} = h(T_m - T_a) \quad \dots 6$$

where  $T_m$  is the temperature of outer surface of mold and  $T_a$  is ambient temperature.

#### Assumptions Made

The following assumptions were made for the formulation of the problem:

- 1-Mold is filled instantaneously.
  - 2-Phase transformation proceeds in one direction: liquid to solid.
  - 3-No convection is present in the liquid metal.
  - 4-Thermal properties of the metal casting for liquid and solid phase are different but constant.
- The density considered variable with temperature.

#### Numerical Solution

After discretization of the whole domain and using the forward difference for the time derivative and the central difference for the spatial second derivative, the approximation resulting in :

$$T_{ijk}^{n+1} = T_{ijk}^n + \frac{K\Delta\tau}{\rho C_p} \left[ \frac{T_{i+1,j,k}^n - 2T_{ijk}^n + T_{i-1,j,k}^n}{\Delta x^2} + \frac{T_{i,j+1,k}^n - 2T_{ijk}^n + T_{i,j-1,k}^n}{\Delta y^2} + \frac{T_{i,j,k+1}^n - 2T_{ijk}^n + T_{i,j,k-1}^n}{\Delta z^2} \right] \quad \dots\dots\dots 7$$

Equation (14) is called the *Forward Time, Centered Space* or FTCS approximation to the heat equation. It can be reduced as:

$$T_{ijk}^{n+1} = (1-6F)T_{ijk}^n + F(T_{i+1,j,k}^n + T_{i-1,j,k}^n) + F(T_{i,j+1,k}^n + T_{i,j-1,k}^n) + F(T_{i,j,k+1}^n + T_{i,j,k-1}^n) \quad \dots\dots\dots 8$$

The FTCS scheme is easy to implement because the values can be updated independently of each other. The entire solution is contained in two loops: an outer loop over all time steps and an inner loop over all interior nodes. Notice that The FTCS can yield unstable solutions that oscillate and grow if  $\Delta\tau$  is too large. According to Jaluria [8], stable solutions with the FTCS scheme are only obtained if;

$$F = \frac{K\Delta\tau}{\rho C_p (\Delta x)^2} \leq \frac{1}{6} \quad \dots\dots\dots 9$$

#### Computer Programming

A computer program has been developed using FORTRAN 90, to carry out the numerical solution, on a personal computer. The basic structure of this program is shown in Fig. 1. Dimensions of casting are illustrated in Figs. 2 and 3.

#### EXPERIMENTAL PROCEDURE

After melting the aluminum alloys in a gas furnace and degassing with a  $C_2Cl_6$  tablets, the molten metals were poured in sand molds. Ten straight bar samples (Fig.2) with different dimensions were prepared to study the effect of silicon percentage on the shrinkage defects. Also, two rectangular samples (Fig.3) with fin were prepared to evaluate the efficiency of the program in prediction the cavities location. All of these samples were contained in Table 1.

#### RESULTS AND DISCUSSION

##### Verification of The Model

In order to check the program, numerical simulation results were compared with experimental data. It conducted by inserting thermocouple in the cast sample (1). Fig.4 shows the simulated and experimental cooling curves at cast center position. It is obvious that the slope of the simulated curve after solidification is smaller than experimental one which may be due to the effect of solid contraction and consequently the air gap development. But, at the interval between the liquidus and solidus temperature (local solidification time), It represents a quite similar between them.

##### The Effect of Si% on The Shrinkage Morphology

Four samples with different silicon percentages are arranged in Table 2. It contains the shrinkage morphologies extracted from Fig. 5. Fig.5d shows that, the pure aluminum (sample 7), suffered from only one type of shrinkage defects. Feeder tends to pipe deeply; the pipe is smooth and geometric in shape, with the absence of any type of shrinkage porosities as shown in Fig. 7. This can be attributed to the plane front

solidification behavior of pure alloys. Two reasons to the severe extent of pipe in these samples. First, the high solidification contraction of pure aluminum (7.14%). Second, the absence of the other types of shrinkages leads to accumulation in the pipe only.

Sample (6) of low silicon content (0.85%) had approximately the same shrinkage behavior as the pure aluminum samples. Here the pipe is less regular and the end is ragged as shown in Fig.5c.

Sample (4) of 7% silicon exhibited light pipe and a dispersed porosity in all cast regions, as shown in Fig.5b and Fig. 6. This is explained by the long freezing range of this composition which offered a high constitutional supercooling and an effective dendritic solidification behavior and consequently a limited feeding to the interdendritic shrinkage regions so that a nucleation of porosities enhanced. On the other hand, the reason of the presence of small pipe in comparison with the previous alloys is firstly; that the total contraction percentage of Al-Si alloys decreases with increasing the silicon content. Secondly; the total contraction here shared between the pipe and wide dispersed porosities.

Sample (1) of 12% silicon (Figs. 5a and 8) exhibited medium size pipe and localized porosities in the centerline. The short freezing range of this alloy produced a simple constitutional supercooling resulted in cellular or light dendritic freezing mode for the eutectic layers or for the aluminum grains which contain the porosities in between. The pipe of this sample is smaller than that of sample (7) because the total contraction percentage of this alloy is 3.8%; also it is larger than that of sample (4) because the porosities here are localized in the centerline only.

### Simulation Results

#### The Pure Aluminum

The first extension of the modeling is the evaluation of the temperature gradient over the mid surface (x-y) of the pure aluminum (7, 8, 9, and 10) samples as in Fig. 9. In general, the gradients are highest at the casting edges, but decrease with moving toward the casting center

characterized by high gradients, whereas the middle regions of thick castings such as sample (9) have very low gradients. All of These samples are free from the porosities in a different manner than steel, i.e. the development of the porosities depends on the decreasing of the temperature gradient under a critical value as the work of Niyama et al [9]. Consequently, the development of the porosities in pure aluminum did not depend on the gradient values because the solidification front type (planar) has the predominant role in this manner and the gradient has no role.

The second extension of the model is to predict the cooling rate during solidification, as shown in Fig.10. The cooling rate is higher near the edges (metal-mold interface) than the casting interior.

The third extension is illustrated in Fig.11 which includes the distribution of the solidus time of sample (9) through the same (x-y) surface. It shows some degree of a directional solidification behavior especially at the casting edges (free edge and near the feeder edge) with stability through a wide intermediate range because of the long casting length.

Among these solidification parameters, the solidification time can be used in the cavities prediction. The appearance of a closed loop in the solidification time contours is the suitable criterion for this type of shrinkage. For checking the efficiency of the present simulation program with employing the solidification time criterion in prediction the cavities position, a rectangular sample designed to produce an internal cavity was tested (sample 11). Fig.12 includes a comparison between the sliced sample (to identify the position of the real cavity) and a simulated graph of the solidus time contours over the same sliced surface. There is a good agreement between them that make this criterion a good tool in cavities prediction and a successful of the present computer program in the simulation function to predict the hot spot and consequently the cavity.

#### Aluminum-0.85% Silicon

Figs. 13a and b show the distribution of the temperature gradient through the mid surface (x-y) for samples (5 and 6). Also, the gradient decreased for very low values and did not cause a development of porosities. Therefore, their solidification behavior resemble to the pure aluminum.

### Aluminum - 7% Silicon

Figs. 5b and 6 include photographs of the polished section of sample (4), which show a wide dispersed of shrinkage porosities through the sample section without any concentration in a specified region. Fig.9a illustrates the distribution of the temperature gradient through the mid surface (x-y). It clarifies that; the shrinkage porosities distribution in this silicon concentration does not depend on this parameter values, and they can not be predicted with this tool.

### Aluminum-12%Silicon

Fig.13d shows the distribution of the temperature gradient through (x-y) mid surface of samples (2). The temperature gradients near the wall area are high due to rapid wall chilling.

Table 3 contains the values of the porosity length extensions in these samples in addition to the gradient values at the starting and ending points. The region of shrinkage coincides with the region of shallow temperature gradient (center line shrinkage). In fact, all of the shrinkage porosities were found within the region of calculated temperature gradient of lower than 1.3 °C/cm. Therefore, 1.3 °C/cm was tentatively taken as the critical value of shrinkage occurrence. The equivalence of these values at the two points for a one sample and between the three different dimensions samples gives a good support for this proposal. Niyama et al [9] reported the values of the critical temperature gradient; 2 to 3°C/cm for the steel bars. The difference between Niyama values and ours is not surprising because the values must depend on casting type, alloy composition. Niyama did not take into account the change in thermal properties for liquid and solid. While Niyama's criterion works well for low carbon steel, that has very small difference between solid and liquid properties that makes its application by many nonferrous foundries is questionable because they have large diverge of thermal properties between solid and liquid metal.

Fig.14 shows the microstructure of eutectic layers, the aluminum grains and porosities. There are characteristic phenomena in the relation between the porosity and the eutectic layers. Firstly; the interlamellar eutectic distance is refined for a high values adjacent to the porosities. Secondly; the eutectic layers surfaces around the porosities are mainly perpendicular to the surface of the porosities. These phenomena may be attributed to the mechanical waves resulted from the bursting initiation of shrinkage porosities, that enhances the nucleation process of the eutectic phase starting from the porosity surface and growing outside vertically.

## CONCLUSIONS

From the present work, the main conclusions can be summarized as:

- 1-The shrinkage porosities increase with increasing the Si content up to 7%, so at this peak, they spread in all cast regions and cannot be predicted.
- 2- The low Si and pure Al-alloys castings suffered from the shrinkage cavities defects only which can be predicted by mapping the solidus time contours.
- 3- The critical temperature gradient value of the shrinkage porosities development in the eutectic (Al-12%Si) alloys was 1.3 °C/cm.

## REFERENCES

- 1- Beckermann, "Modeling of Solidification", Purdue Heat Transfer Celebration, April 3-5 University of Iowa, pp. 19-22, 2002.
- 2- M. Trovati and S. A. Argyropoulos, "Mathematical Modeling and Experimental Measurement of Shrinkage In The Casting of Metals", Canadian Metallurgical Quarterly, Vol.35, pp. 77-84, 1996.
- 3- M. Bride, "Numerical Simulation of Incompressible Flow Driven By Density Variation During Phase Change", Int. J. Numer. Meth. Fluids, Vol.3.1, pp. 787-800, 1999.
- 4- C. Kim and S. Ro, "Shrinkage Formation during the Solidification Process in an Open Rectangular Cavity", ASME, J. Heat Transfer, Vol. 115, pp. 1078-1081, 1993.
- 5- U. Andrause and F. Delli'isola, "On thermokinematic Analysis of Pipe Shaping in Cast Ingot: A Numerical Simulation via FDM", Int. J. Engng. Sci., Vol. 34, pp. 1349-1367, 1996.

- 6- M. Paszndiden-Fard, "A Three Dimensional Model of Droplet Impact and Solidification", J. Heat Mass Transfer, Vol. 45, pp. 2229-2242, 2002.
- 7- D. Poirier and M. Salcudean, "On Numerical Methods Used in Mathematical Modeling of phase Change in Liquid Metals", Transaction Heat Transfer, (1988).
- 8- Y. Jaluria, "Computer Methods for Engineering", Allyn and Bacon Inc., USA, 1988.
- 9- E. Niyama , T. Uchida, M. Morikawa and S. Saito, "A Method of Shrinkage Predicting and Its Application to Steel Casting Practice", 49<sup>th</sup>, International Foundry Congress, p.1, 1982.

## NOMENCLATURE

**T** : temperature  
**C<sub>p</sub>** :thermal capacity  
**K** :thermal conductivity  
**q\*** :heat generation  
**L** :latent heat  
**f<sub>s</sub>** : solid fraction  
**f<sub>l</sub>** :liquid fraction  
**P** : Property  
**h** :heat transfer coefficient  
**ρ** :density  
**τ** : time

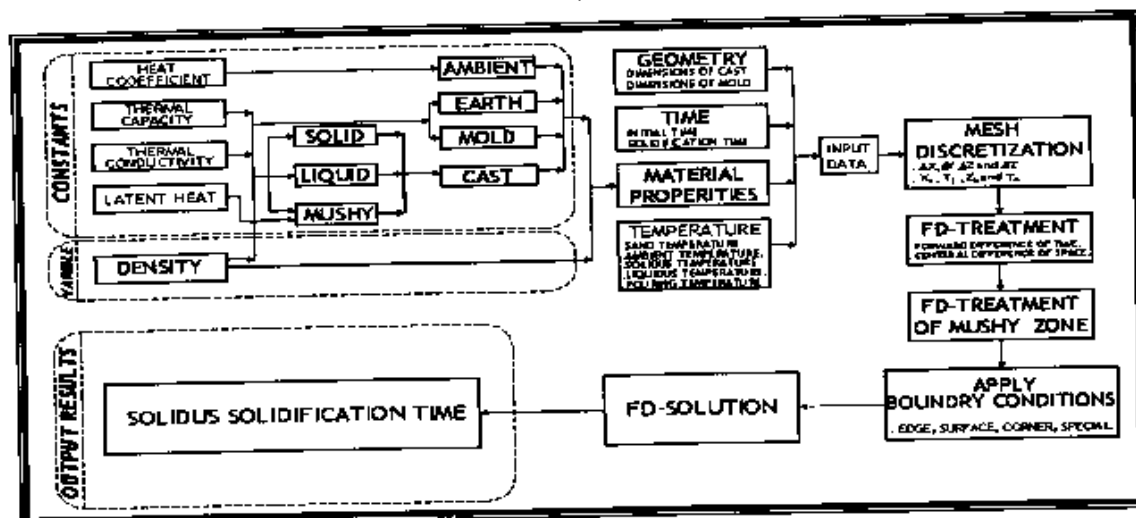


Fig.1 basic structure of FD-program

Table 1 dimension of the casting samples

SP. No.	CAST METAL	CAST LENGTH (mm)	CAST WIDTH (mm)	CAST THICKNESS (mm)	FEEDER LENGTH (mm)	FEEDER DIAMETER (mm)	POURING TEMP. (°C)	SOLIDUS TEMP. (°C)	LIQUIDUS TEMP. (°C)
1	Al-12%Si	500	50	30	145	45	610	542	573
2	Al-12%Si	520	35	30	145	45	610	542	573
3	Al-12%Si	480	70	30	145	45	610	542	573
4	Al-7%Si	470	45	30	145	45	650	567	614
5	Al-0.85%Si	480	45	30	145	45	690	643	648
6	Al-0.85%Si	380	40	30	145	45	690	643	648
7	Pure Aluminum	500	50	30	145	45	705	660	660
8	Pure Aluminum	530	40	30	145	45	705	660	660
9	Pure Aluminum	520	35	30	145	45	705	660	660
10	Pure Aluminum	460	45	30	145	45	705	660	660
11	Pure Aluminum	100	60	30	-	-	705	660	660
12	Al-12%Si	100	60	30	-	-	610	542	573



Fig.2 straight bar samples

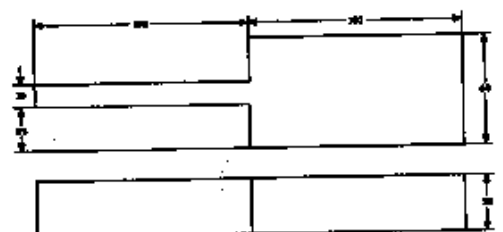


Fig.3 rectangular samples

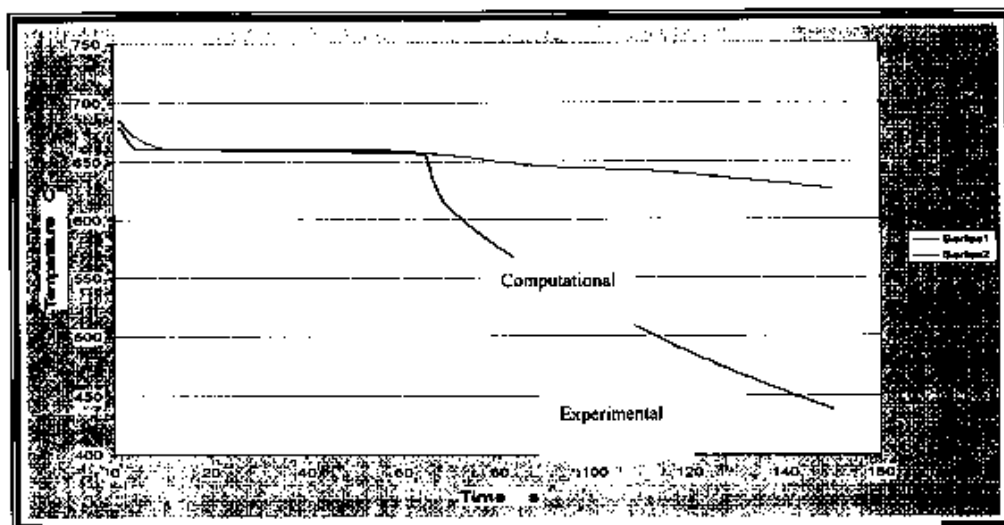


Fig.4 comparison between simulated and experimental results at the centre of the cast (1)

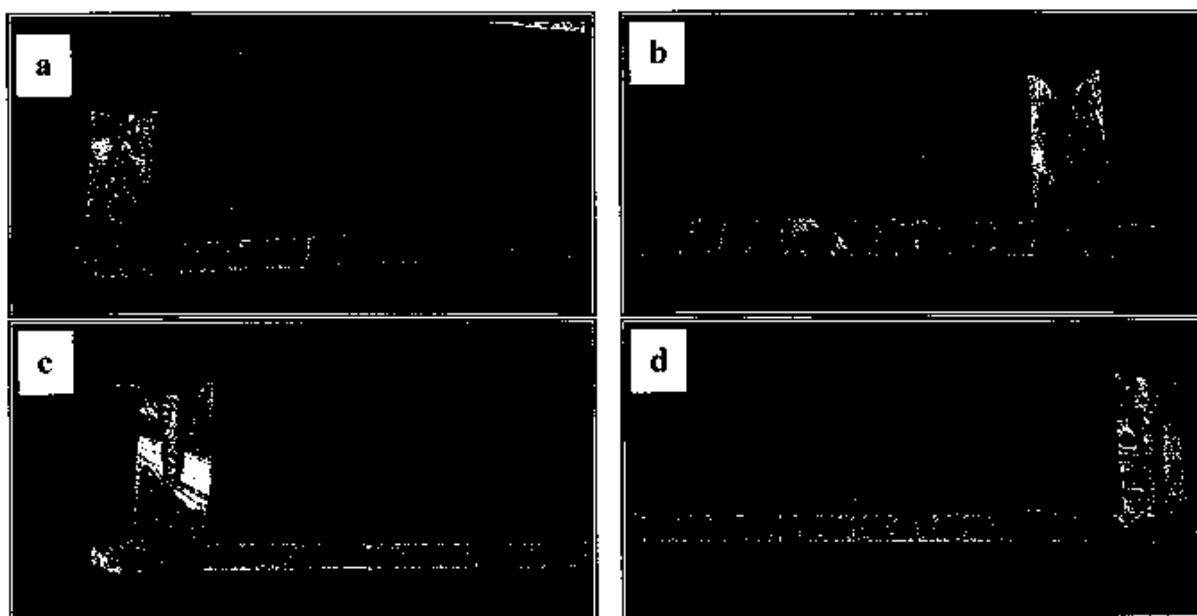


Fig.5 photographs of a-sample(1), b-sample(4), c-sample(6), and d-sample(7) sections, which illustrate the shrinkage defect morphologies



Table 2 shrinkage defect morphologies of the casting samples

Sample code	Si %	Pipe	Centerline porosities	Dispersed Porosities	Surface sink
1	12	medium	present	nil	nil
4	7	light	nil	severe	nil
6	0.85	severe	nil	nil	present
7	0	severe	nil	nil	nil

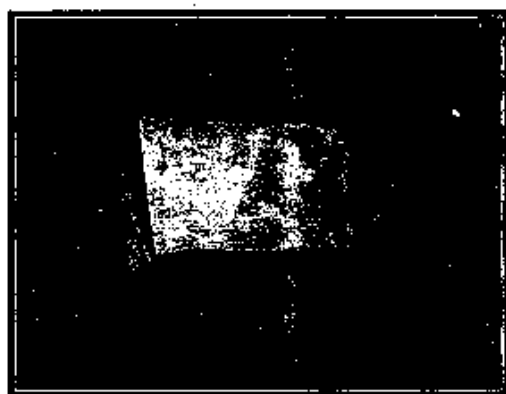


Fig. 6 a photograph of polished section of sample (4) shows the dispersed porosities

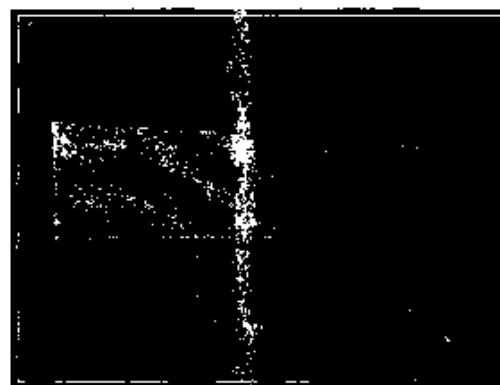


Fig. 7 a photograph of polished section of sample (7) shows the porosity free surface

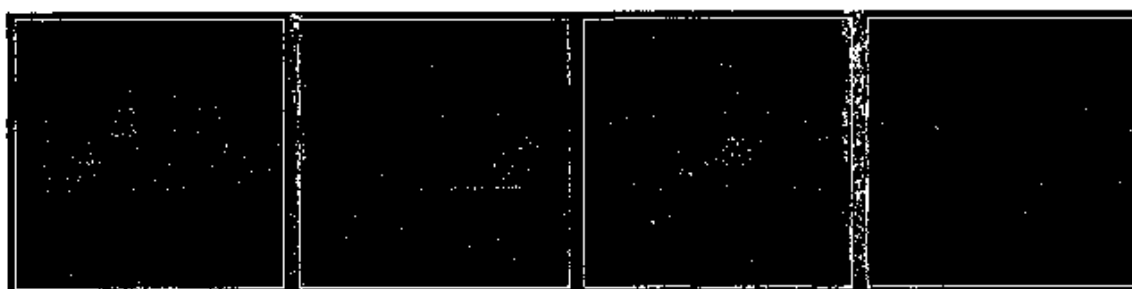


Fig. 8 a photograph of polished section of sample (1) shows the centerline porosities

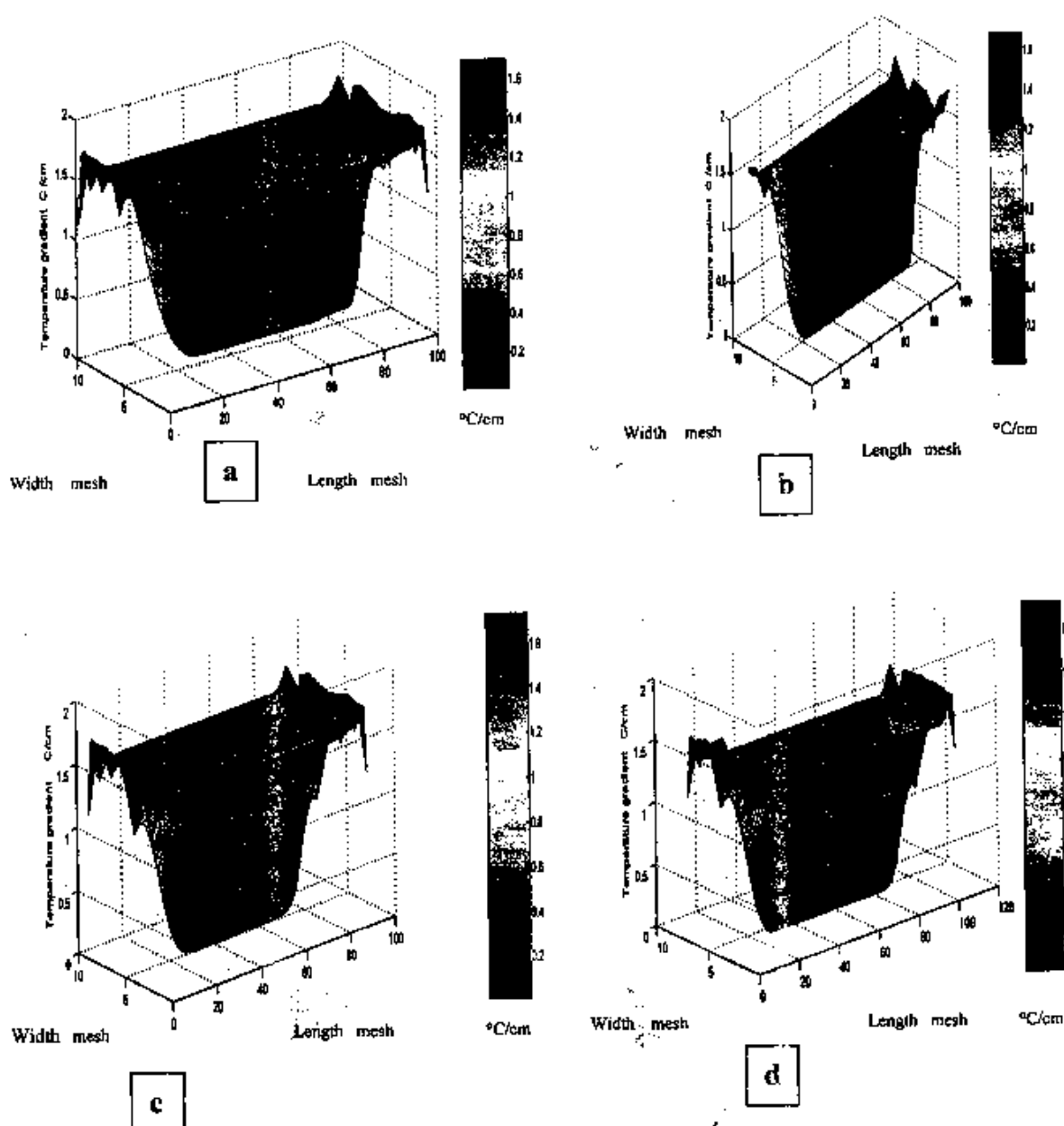


Fig.9 the temperature gradient variation over the mid surface of a-sample (7), b- sample (8), c- sample (9), and d- sample (10)

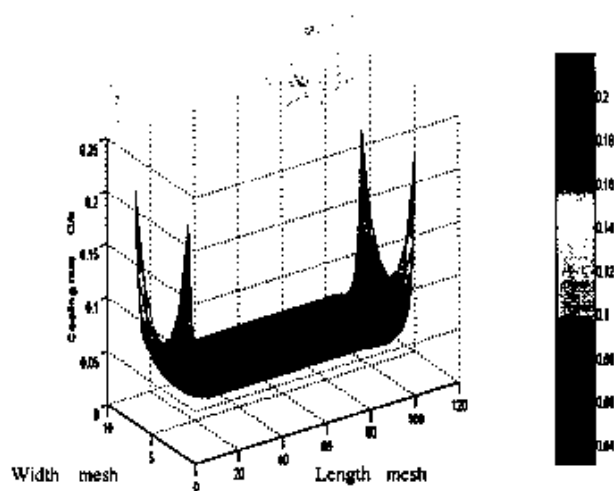


Fig.10 the Cooling rate over the mid surface of sample (9)

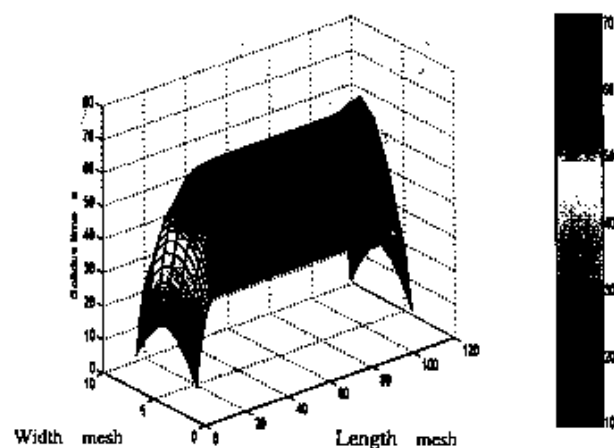


Fig. 11 the solidus time variation over the mid surface of sample (9)

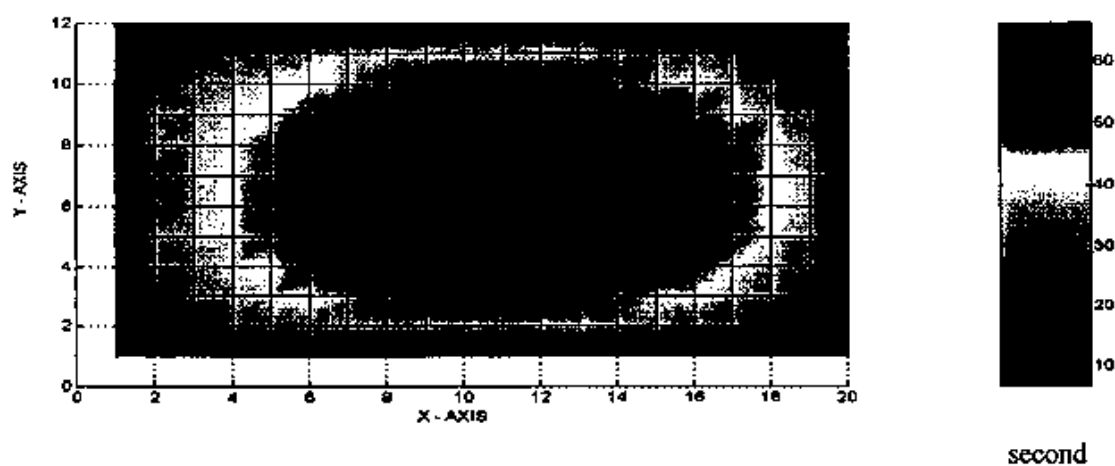
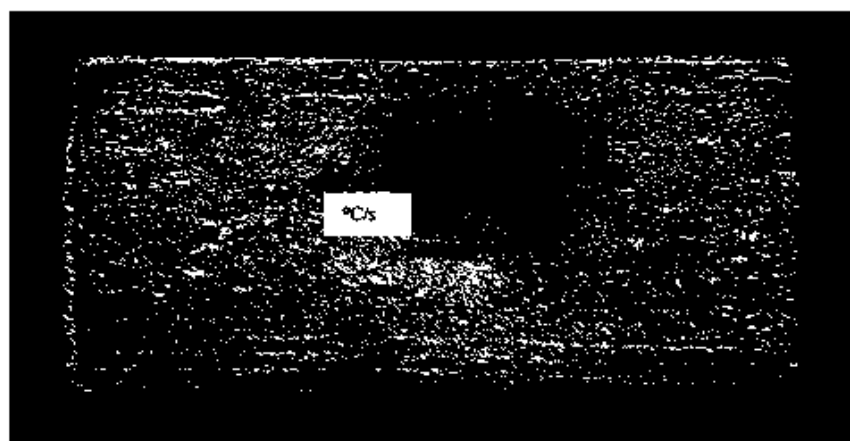


Fig. 12 the solidus time contours over the mid surface of sample (11)

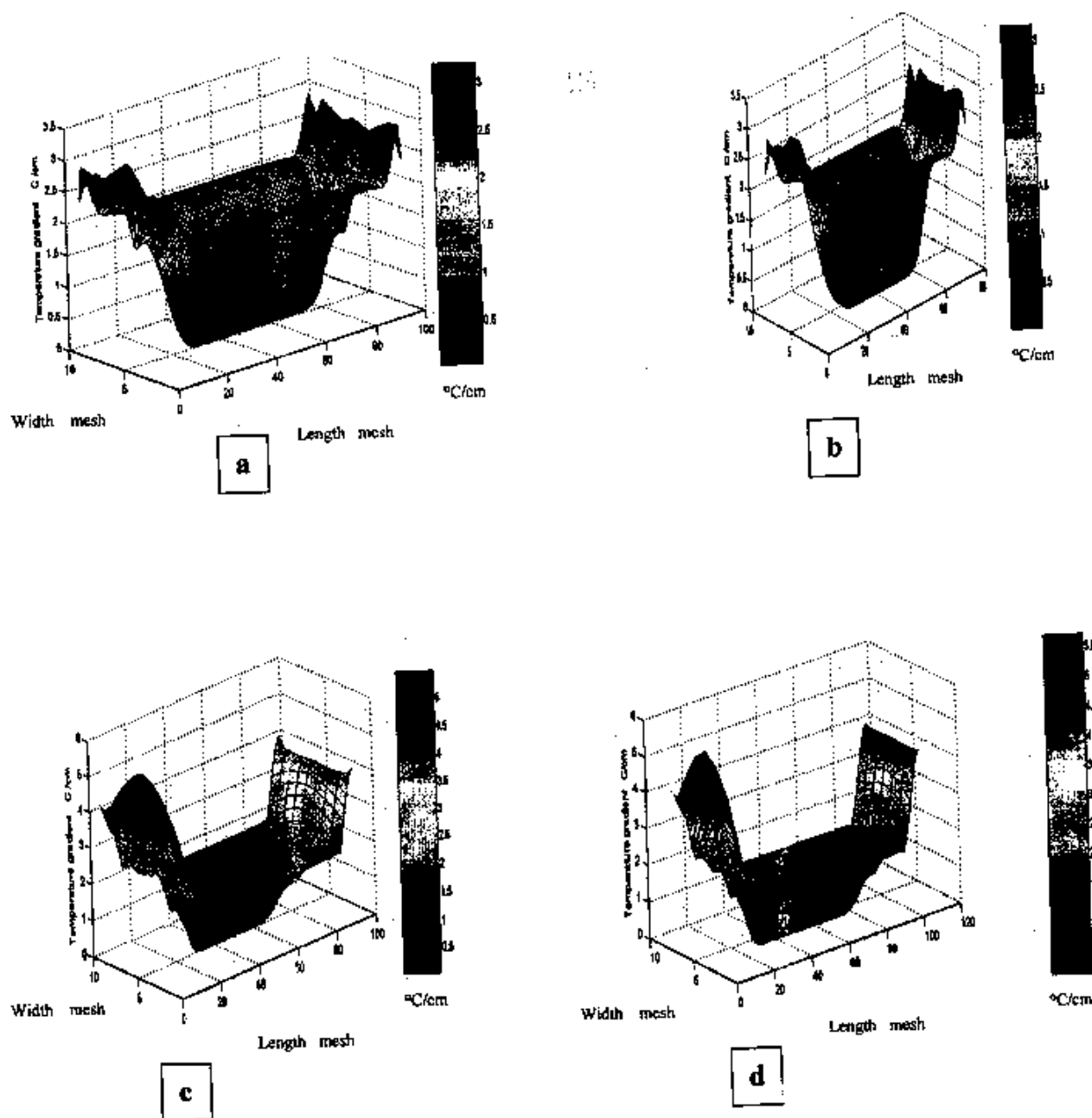
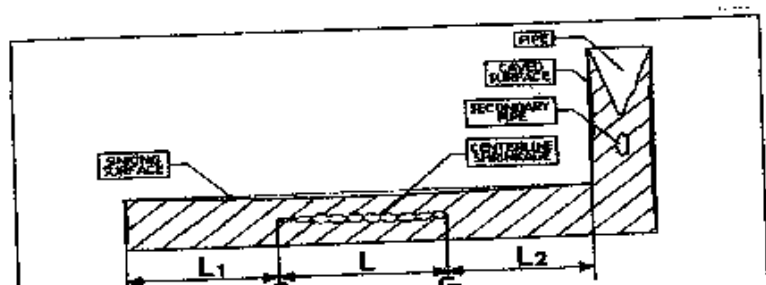


Fig. 13 the temperature gradient variation over the mid surface of a-sample (5), b- sample (6), c- sample (4), and d- sample (2)

Table 3 values of critical temperature gradients which is gained from simulation



TEST No	CAST METAL	CAST LENGTH (L) (mm)	CAST THICKNESS (T) (mm)	CAST WIDTH (W) (mm)	END EFFECT (L1) (mm)	CENTERLINE SPRING (L2) (mm)	FEEDER EFFECT (L3) (mm)	EDGE TEMP. GRADIENT (G1) °C/mm	EDGE TEMP. GRADIENT (G2) °C/mm
1	AL-12SI (LAI3)	500	30	50	120	320	60	1.34	1.31
2	AL-12SI (LAI3)	520	30	35	100	350	70	1.35	1.3
3	AL-12SI (LAI3)	480	30	70	140	255	85	1.34	1.38

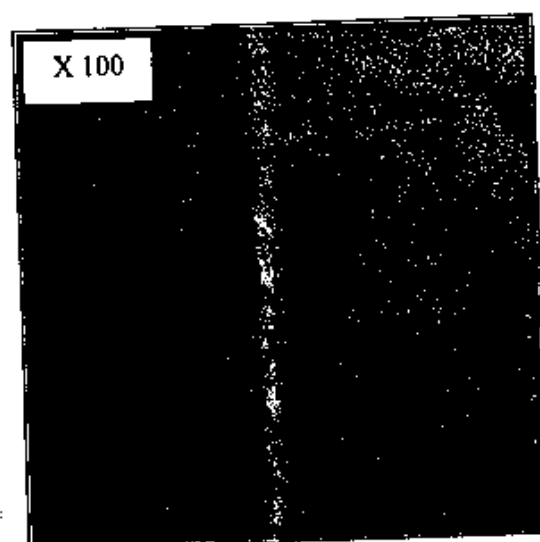
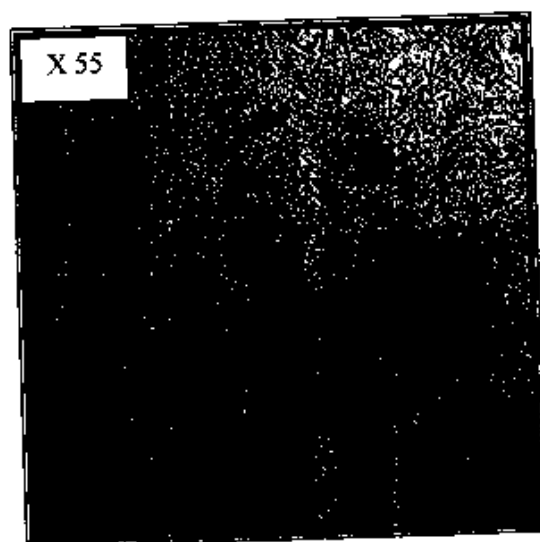


Fig.14 micrographs with two magnifications of the microstructure of sample (1) showing the refining of eutectic layers around the porosities